THE STEREOSCOPIC DETERMINATION OF THE BLUNTING LINE

O. Kolednik, H.P. Stüwe*

Several precracked CT-specimens of an annealed structural steel were loaded to different amounts of crack-tip blunting at room temperature, and subsequently broken in liquid nitrogen. The relationship between formation of the stretched zone and the J-integral is studied with the method of stereophotogrammetry using a scanning electron microscope. A new accurate method of determining J_{IC} is proposed.

INTRODUCTION

The critical value of the J-integral, J_{IC}, is found as the point on the J-resistance-(R-)curve, i.e. a curve J versus crack extension Δa, at the moment of initiation of stable crack growth. This point of crack initiation is determined by intersecting the stable-tearing line of the R-curve with the blunting line, which corresponds to the blunting of the crack tip, and to the formation of the stretched zone during the first stages of loading.

In the ASTM-standard for J_{IC}-testing (1), a so-called "theoretical blunting line" is given as

$$J = 2 \cdot \sigma_F \cdot \Delta a \qquad (1)$$

where σ_F represents an "effective flow stress" which allows for the work hardening of the material during the blunting process. Following (1) σ_F is given as the average of the yield strength σ_y and the ultimate tensile strength σ_u

$$\sigma_F = \frac{1}{2}(\sigma_y + \sigma_u) \qquad (2)$$

Eq. 1 seems to be in good agreement with experimental results for many materials (2,3). However, especially for low-strength and high strain-hardening materials, Eq. 1 overestimates the crack extension due to blunting (3,4,5), which can result in non-conservative J_{IC}-values. Therefore it is important to establish an accurate blunting line for these materials.

*both Erich-Schmid-Institut für Festkörperphysik der Österreichischen Akademie der Wissenschaften, Jahnstr. 12, A-8700 Leoben, Austria.

The theoretical foundation of Eq.1 is based on the relationship between J and the crack-tip-opening displacement

$$J = m \cdot \sigma_y \cdot COD \qquad (3)$$

and on the correlation between crack extension Δa and COD

$$\Delta a = n \cdot COD \qquad (4)$$

Before the initiation of stable crack growth, the crack extension Δa should be equal to the width of the stretched zone SZW. The factor m in Eq. 3 depends mainly on the strain-hardening exponent N of the material.

Many theoretical investigations have been concerned with the two relationships above, primarily with Eq. 3 (6,7), but their experimental verification is poor. This is caused by the great difficulties in measuring COD and its critical value COD_c.

In this work we studied the relationship between J-integral and the formation of the stretched zone to determine the factors m and n of the two equations and to derive an accurate mathematical formulation of the blunting line.

EXPERIMENTAL

Material

The material investigated was a structural steel. Test pieces were austenized at 870°C for 45 minutes, quenched in salt water, tempered at 700°C for 4 hours and furnace cooled down to 500°C at a rate of 2 degrees per minute. Compact tension (CT-) specimens were machined, with a thickness B = 25 mm and a short-transverse crack-plane orientation.

The microstructure had small carbide particles embedded in a ferrite matrix with a great number of MnS-inclusions parallel to the crack front. The chemical composition of the steel and its conventional mechanical properties at room temperature (RT) are given in Tab. 1.

On two specimens a J_{IC}-single-specimen test was conducted where the physical crack length was determined by partial unloading (8)*. The two specimens gave J_{IC}-values of 51 and 53 kJ/m^2. The R-curve of one of these tests is shown in Fig. 1.

Table 1 - Chemical composition and mechanical properties

C	Mn	Si	P	S	Ni	Cr	Mo	Cu	As
0.17	0.54	0.01	0.019	0.018	0.04	0.01	0.01	0.01	0.002

Yield strength	Tensile strength	Youngs modulus	work-hardening coefficient
σ_y = 298 MNm^{-2}	σ_{UTS} = 426 MNm^{-2}	E = 200 GNm^{-2}	n = 0,20

*These tests were performed by P. Uggowitzer at the Institut für Metallurgie, ETH Zürich, Switzerland

At the temperature of liquid nitrogen (-196°C) a tensile test gave a fracture strength of $\sigma_u^{(N)}$ = 990 MN/m^2 without any plastic straining.

R-curve

The CT-specimens were precracked in fatigue. During the final stages of crack extension the maximum stress intensity of the fatigue cycle was 17,6 ± 0,3 MN/m$^{3/2}$. Five specimens were loaded to different amounts at RT and subsequently broken in liquid nitrogen. They failed in a ductile tearing mode at RT, but in a transgranular cleavage mode at low temperatures. This change of the failure mode allowed an accurate observation of the formation of the stretched zone.

The load versus load-line-displacement curve (F - v_L-curve) of specimen 6 at RT is shown in Fig. 2, in addition the maximum loads of the other specimens are included. The area under the F-v_L-curves was used to determine the values of the J-integral. Another specimen was broken without pre-loading to determine the sharpness of the fatigue crack. The test gave a valid value of $K_{IC}^{(N)}$ = 29,6 MN/m$^{3/2}$.

The crack extension was determined at nine equidistant positions along the crack front by means of micrographs from a scanning electron microscope (SEM). From each micrograph three measurements were made of SZW and of the stable-tearing-crack extension.

From our J-R-curve, Fig. 3, we can conclude that the initiation of stable fracture must occur somewhere between the points 5 and 6. The "theoretical blunting line" does not agree with the data points.

Stereoscopic measurements

Stereoscopic measurements have been shown to be a very efficient method to determine COD with a high accuracy (9,10), but it is essential to analyse the corresponding regions on both specimen halves to lower drastically the scatter of the individual COD-values (11). This idea of measuring on both specimen halves was already applied successfully for estimates of the plastic work, which is necessary to form a ductile fracture surface (12,13,14).

Determination of the sharpness of the fatigue crack. Fig. 4a shows a transition region from fatigue to cleavage fracture in the centre of specimen 1 , Fig. 4b presents the corresponding region on the second specimen half. From these corresponding regions we produced stereo-image pairs in the SEM by the tilting method. On each photogram a profile was analysed point by point with a stereo comparator. Subsequently a FORTRAN program was used to calculate the coordinates of the analysed points relative to a reference plane. The method is described in detail in (15), also an estimate of the accuracy is given. The shape of the profiles between the calculated points was sketched by means of the stereo comparator, too.

To determine COD at the moment of crack initiation we try to reconstruct the position of the profiles at the moment of crack initiation. We look for two corresponding points on the profiles, e.g. point 9 on profile 1 corresponds to point 9 on profile 2 (compare with the micrographs Fig. 4a and Fig. 4b).

Therefore these two points have to match. The profiles are shifted parallel to the point where they merge in the region of cleavage fracture (Fig. 4c). So we get COD(N)=1µm and an upper limit of 0,5µm for the radius of the fatigue crack.

Stretched zones In the same way as mentioned above we analysed the regions of the stretched zone in the centre of the other specimens. The blunting of the crack tip and the process of void-nucleation and -growth at the position of the most effective MnS-inclusion in front of the crack tip is depicted in Fig. 5a - e. Fig. 5e shows the moment of initiation of the stable crack growth, i.e. when the first void coalesces with the blunted crack tip.

According to Dawes (16), COD should be measured at the position of the tip of the fatigue crack before loading, i.e. at the boundary between the fatigue crack and the stretched zone. As an example, for the profile A of specimen 6 this boundary is located between the points 4 and 5 (Fig. 6). In general it is necessary to look for these points on both of the corresponding profiles (11).

DISCUSSION

The scatter of the COD-values

This subject was already discussed in detail in a preceding paper (11). In this work another specimen of the same material was loaded until some stable crack growth occurred. Eight profiles of the stretched zone region in the centre of the specimen were analysed to determine the critical COD. The scatter of the individual COD_c-values was surprisingly small: $COD_c = 73 \pm 6\mu m$.

Therefore, it was sufficient for the current work to analyse COD at three positions in the centre of each specimen. The COD_c - values of specimen 6 fall well within the scatterband given above (see Fig. 8).

The J-COD-curve and the correlation between Δa and COD

In Tab. 2 the values of the J-integral and the mean values

Table 2 - The relationship between J-integral and the formation of the stretched zone

	Number of Specimen						Values
	1	2	3	4	5	6	from [11]
J [kJ/m²]	2	12,7	18,7	23,7	30,4	41,3	158
SZW [µm]	0	6,0	10	11	11	20	21
Δa [µm]	0	7,2	13	15	22	67	454
COD [µm]	1	15	27	38	57	71	73

of SZW, crack extension and COD are listed. The data from (11) are given, too. Although there is no relationship between the individual values of COD and Δa on one position of the specimen (11), a reasonable correlation could be found between COD and the mean value of Δa (Fig. 7).

$$\Delta a = 0{,}42 \cdot COD \qquad (4)$$

As Fig. 8 indicates, there is a very good correlation between J and COD. Inserting the material's yield strength we get

$$J\,[kJ/m^2] = 4\,[kJ/m^2] + 480\,[MN/m^2] \cdot COD\,[m] \qquad (5)$$

The mathematical formulation of the blunting line is estimated by combining Eq. 4 and Eq. 5 (Fig. 3).

$$J\,[kJ/m^2] = 4\,[kJ/m^2] + 1150\,[MN/m^2] \cdot \Delta a\,[m] \qquad (6)$$

The question remains still unanswered to what extent the relationships given above are valid for other low-strength materials. It does not seem reasonable to relate the slope of the blunting line to the "effective flow stress" σ_F, because a real mean flow stress during the blunting process must be much higher than σ_F (17). An estimate of a mean flow stress is given in (13).

A new method to determine J_{IC}

From the relationship between J and COD we can easily determine J_{IC} by extrapolating the line to the value of the critical COD_c (Fig. 8). It can be seen that J_{IC}, measured by the single-specimen-compliance method is too high by 33 percent.

So we can propose another method to determine J_{IC}: One specimen is loaded until some stable crack growth occurs. From this specimen the critical value COD_c is analysed. The second specimen is monotonically loaded below the critical point, e.g. specimen 5 in Fig. 8, then it is cooled down or post-cracked in fatigue to mark the amount of stretched-zone formation, and subsequently broken. By measuring J and analysing COD we get the J-COD-relationship in Fig. 8 and by extrapolating the line to COD_c we can determine J_{IC}.

The major advantage of this method lies in the fact that it permits an exact determination of the initiation of stable crack growth and, therefore, a very accurate measure of J_{IC}.

ACKNOWLEDGEMENT

The authors would like to thank Dr. P. Uggowitzer at the Institut für Metallurgie, ETH Zürich, Switzerland, for performing the J_{IC}-single-specimen tests and for helpful discussions.

SYMBOLS USED

Δa	=	crack extension
B	=	specimen thickness
COD	=	crack-tip-opening displacement
COD_c	=	critical value of crack-tip-opening displacement
$COD\ (N)$	=	crack-tip-opening displacement at - 196°C
F	=	load
J	=	value of the J-integral
J_{IC}	=	critical value of the J-integral
$K_{IC}(N)$	=	plain-strain-fracture toughness at -196°C
m	=	factor in the relationship between J and COD
N	=	strain-hardening exponent
n	=	factor in the relationship between Δa and COD
SZW	=	stretched-zone width
v_L	=	load-line displacement
σ_F	=	"effective" flow stress
σ_u	=	ultimate tensile strength
$\sigma_u(N)$	=	ultimate tensile strength at -196°C
σ_y	=	yield strength

REFERENCES

1. Standard Test Method for J_{IC}, a Measure of Fracture Toughness, ASTM E 813-81, Annual Book of ASTM-Standards, Part 10
2. Robinson, J.N., and Tetelman, A.S., in ASTM STP 559, (1974) 139
3. Mills, W.J., Journal of Testing and Evaluation,9, (1981) 56
4. O'Brian, D.M., and Ferguson, W.G., Int. Journ. of Fracture,20,(1982) R 39
5. Yin, S.-W., et al., Engng. Fracture Mech.,18,(1983) 1025
6. Shih, C.F., J. Mech. Phys. Solids,29,(1981) 305
7. McMeeking, R.M., J. Mech. Phys. Solids,25,(1977) 357
8. Uggowitzer, P., and Sigrist, P., Berg- und Hüttenmänn. Monatshefte,128,(1983) 72
9. Broek, D., Engng. Fracture Mech.,6,(1974) 173
10. Krasowsky, A.J., and Vainshtok, V.A., Int. Journ. of Fracture,17,(1981) 579
11. Koledník, O., and Stüwe, H.P., Engng. Fracture Mech. in press
12. Stüwe, H.P., Engng. Fracture Mech.,13,(1980) 231
13. Stüwe, H.P., in "Three Dimensional Constitutive Relations and Ductile Fracture",(North-Holland Publishing Company, 1981, 213)
14. Koledník, O., and Stüwe, H.P., Z. Metallkde.,73, (1982) 219
15. Koledník, O., Practical Metallography,18,(1981) 562
16. Dawes, M.G., in ASTM STP 668,(1979), 307
17. Willoughby, A.A., et al., Int. Journ. of Fracture, 17,(1981) 449

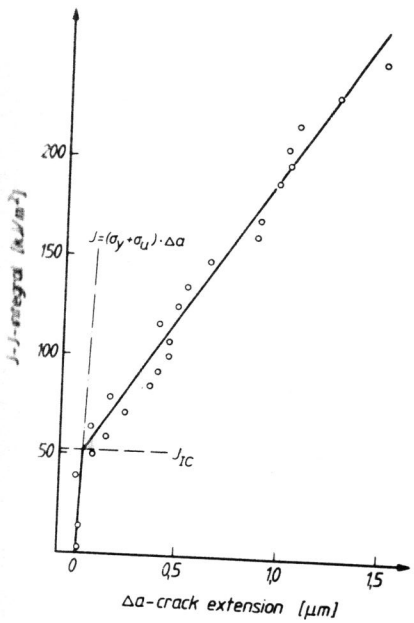

Figure 1 - Result of the J_{IC}-single-specimen test

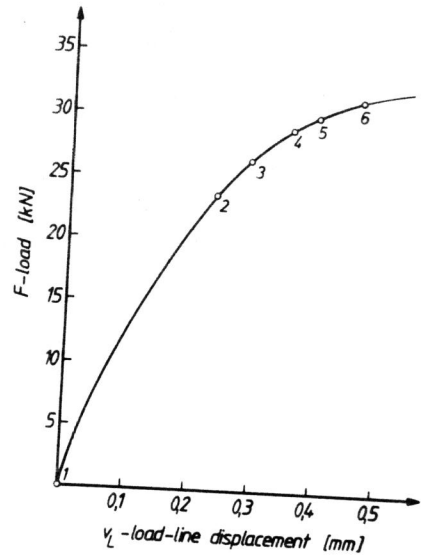

Figure 2 - The relation of load versus load-line displacement of specimen 6 with the maximum loads of the other specimens inserted

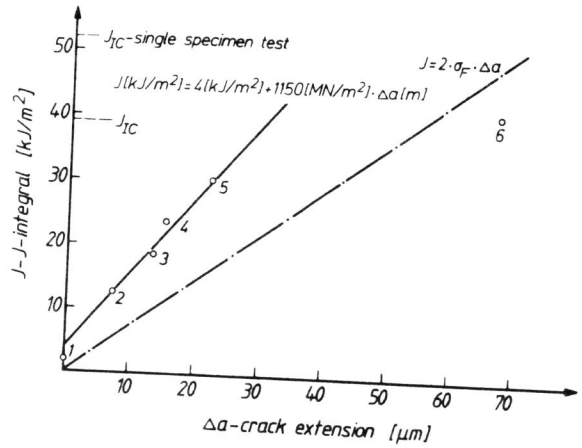

Figure 3 - J-resistance curve in the region of crack-tip blunting

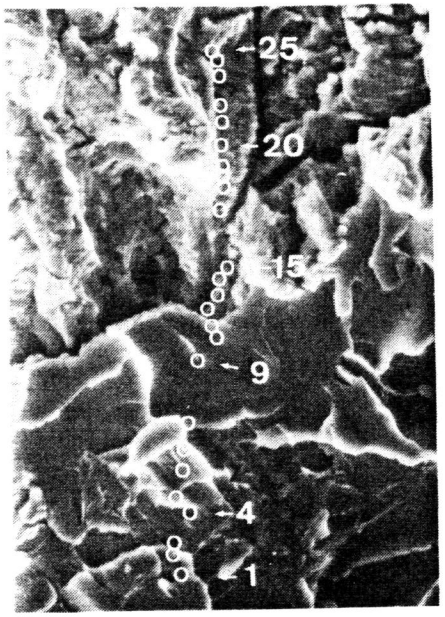

Figure 4a

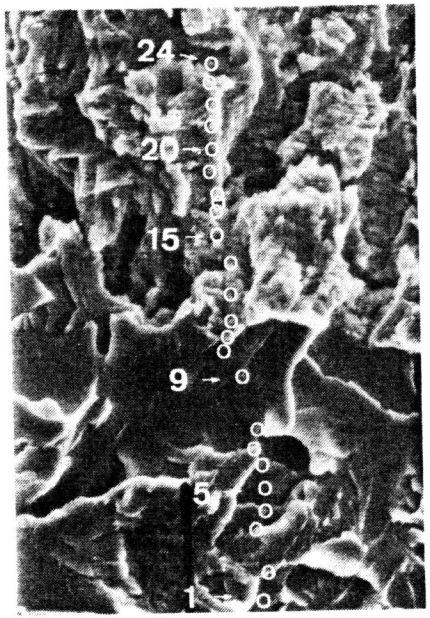

Figure 4b

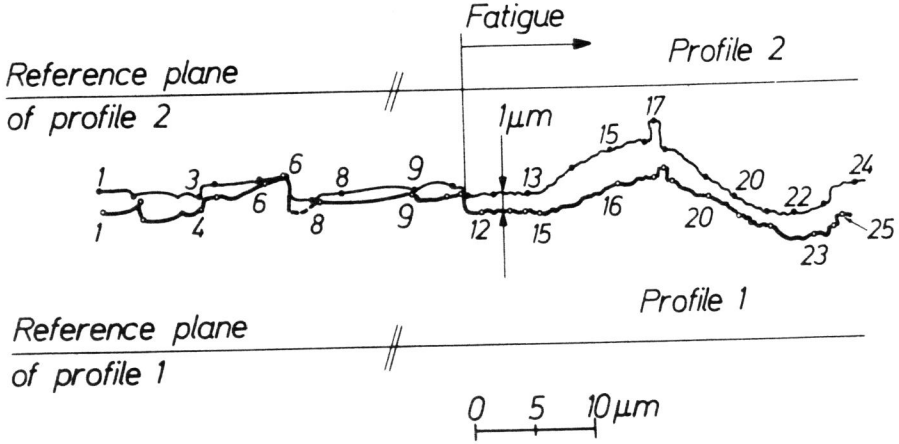

Figure 4c

Figure 4 - Corresponding stretched-zone regions of specimen 1, broken under liquid nitrogen, a) side 1, b) side 2, c) section at the moment of crack initiation

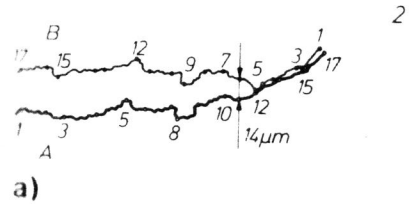

a)

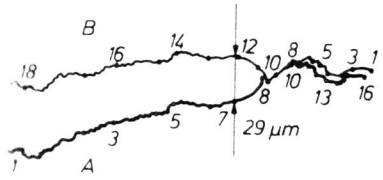

b)

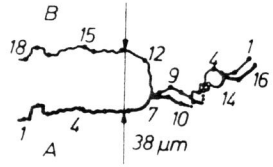

c)

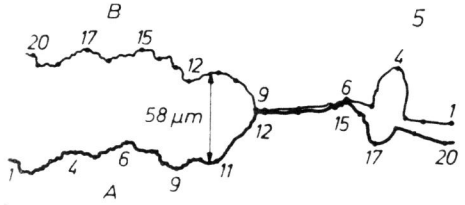

d)

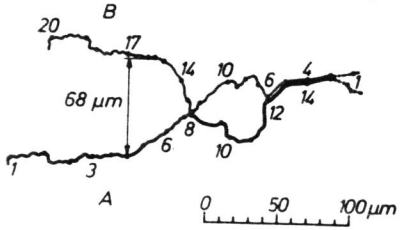

e)

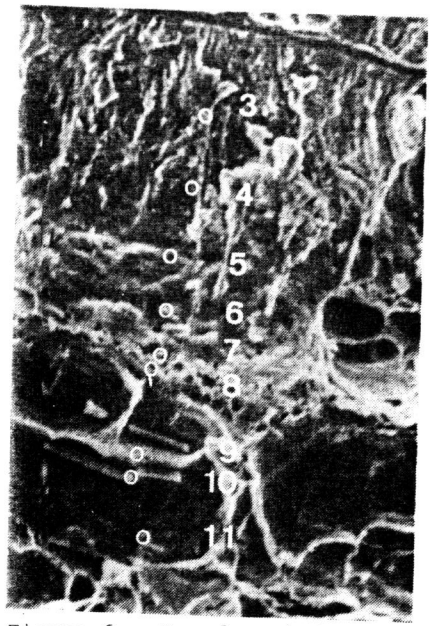

Figure 6 - Boundary between fatigue crack and stretched zone on side A of specimen 6

← Figure 5 - Sections of the corresponding stretched-zone regions of the specimens 1 to 6

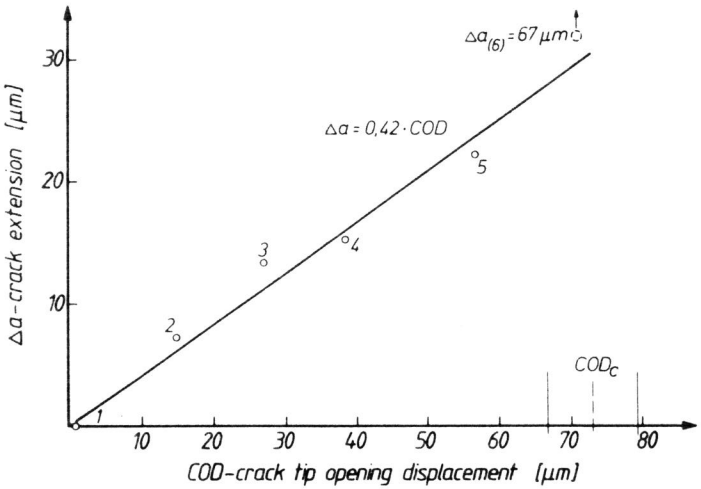

Figure 7 - Correlation between crack extension and crack-tip-opening displacement

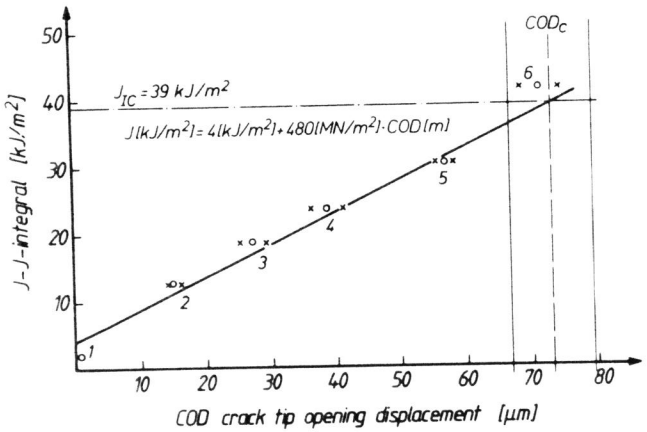

Figure 8 - Relationship between J-integral and crack-tip-opening displacement during the blunting process